Solving the Boltzmann equation to obtain electron transport coefficients and rate coefficients for fluid models

INSTITUTE OF PHYSICS PUBLISHING PLASMA SOURCES SCIENCE AND TECHNOLOGY
Plasma Sources Sci. Technol. **14** (2005) 722–733 doi:10.1088/0963-0252/14/4/011

Solving the Boltzmann equation to obtain electron transport coefficients and rate coefficients for fluid models

G J M Hagelaar and L C Pitchford

Centre de Physique des Plasmas et de leurs Applications de Toulouse,
Université Paul Sabatier, 118 route de Narbonne, 31062 Toulouse Cedex 9, France

Received 13 June 2005
Published 5 October 2005
Online at stacks.iop.org/PSST/14/722

Abstract
Fluid models of gas discharges require the input of transport coefficients and rate coefficients that depend on the electron energy distribution function. Such coefficients are usually calculated from collision cross-section data by solving the electron Boltzmann equation (BE). In this paper we present a new user-friendly BE solver developed especially for this purpose, freely available under the name BOLSIG+, which is more general and easier to use than most other BE solvers available. The solver provides steady-state solutions of the BE for electrons in a uniform electric field, using the classical two-term expansion, and is able to account for different growth models, quasi-stationary and oscillating fields, electron–neutral collisions and electron–electron collisions. We show that for the approximations we use, the BE takes the form of a convection-diffusion continuity-equation with a non-local source term in energy space. To solve this equation we use an exponential scheme commonly used for convection-diffusion problems. The calculated electron transport coefficients and rate coefficients are defined so as to ensure maximum consistency with the fluid equations. We discuss how these coefficients are best used in fluid models and illustrate the influence of some essential parameters and approximations.

1. Introduction

Fluid models of gas discharges describe the transport of electrons, ions and possibly other reactive particle species by the first few moments of the Boltzmann equation (BE): (1) the continuity equation, (2) the momentum equation, usually approximated by the drift-diffusion equation and (3) the energy equation, usually only for electrons. Each of these equations contains transport coefficients or rate coefficients which represent the effect of collisions and which are input data for the fluid model [1–4] (see also references therein).

Transport coefficients and rate coefficients may be rather specific for the discharge conditions. In particular, coefficients concerning electrons depend on the electron energy distribution function (EEDF), which in general is not Maxwellian but varies considerably depending on the conditions. For simple conditions (swarm experiments) and common gases, the electron transport coefficients and rate coefficients have been measured and tabulated as functions of the reduced electric field E/N (ratio of the electric field strength to the gas particle number density) [5].

In general, the EEDF and the electron coefficients for the given discharge conditions can be calculated from the fundamental collision cross-section data by solving the electron BE [6]. A common approach is to solve some approximation of the BE for a series of reduced electric-field values and to put the resulting coefficients in tables versus the reduced field or versus the mean electron energy (disregarding the field values), which are then used in the fluid model to find the transport coefficients and rate coefficients by interpolation. Fluid models without electron energy equation treat the electron coefficients as functions of the local reduced field; models with an electron energy equation treat them as functions of the local mean electron energy.

The BE solvers used to generate the electron-related input data for fluid models are usually based on techniques developed during the 1970s and 1980s, when much work was done on the solution of the BE for the purpose of checking the consistency

between cross-section data and transport coefficients or rate coefficients measured in different experiments [7–16]. These solution techniques originally aimed at simulating specific experiments and calculating the exact physical quantities measured in these experiments with high numerical precision. For fluid discharge modelling, however, one has somewhat different objectives:

(1) the BE solver should work over a large range of discharge conditions (reduced electric field, ionization degree, gas composition, field frequency) rather than simulate a specific experiment;
(2) the calculated transport coefficients and rate coefficients should correspond formally to the same coefficients appearing in the fluid equations (moments of the BE) rather than to quantities measured in experiments; note that the literature gives different definitions of the transport coefficients, some of which are not completely consistent with the fluid equations;
(3) the errors in the calculated transport coefficients and rate coefficients should not limit the accuracy of the fluid model; this is a less strict requirement than the extreme precision (e.g. 0.1% in the drift velocity) needed for the cross-section testing of the 1970s and 1980s;
(4) the BE solver should be fast and reliable without ad hoc calculation parameters to adjust.

There exist several user-friendly BE solvers that are often used and cited by authors in the field of fluid discharge modelling; we mention in particular the commercial ELENDIF [13] and the freeware BOLSIG [17], but there are many others. These solvers however were not designed with the above objectives in mind: they can be applied only for a limited range of discharge conditions, are inconvenient to generate the tables of coefficients or are ill-documented (especially the popular BOLSIG), making it difficult to evaluate the appropriateness of their results for fluid modelling. For years we have felt the need for a new BE solver, able to deal with a larger range of discharge conditions, faster, easier to use and paying more attention to a consistent definition of the calculated coefficients. This is the reason why we have recently developed a new user-friendly BE solver and made it freely available to the discharge modelling community under the name BOLSIG+ [18].

In this paper we document BOLSIG+ in detail. We discuss its physical approximations, numerical techniques, calculated transport coefficients and rate coefficients, and how to use these coefficients in fluid models. In doing so, we provide an extensive discussion on the topic of solving the BE to obtain input data for fluid models. We believe that this is extremely useful: although the techniques used by BOLSIG+ and described in this paper may be well known to BE specialists, developers and users of fluid models are often not aware of them and have little feeling for the precision of the calculated coefficients. The existing literature on BE calculations is so specialized, focusing on specific details, that it is hard to see the consequences for fluid models. This paper looks at the BE from the point of view of a fluid modeller.

2. Boltzmann equation solver

In the following sections we document the physical assumptions and numerical techniques used by our BE solver. We indicate the relation with previous work without trying to be exhaustive; the literature on the electron BE in this context is vast.

The BE for an ensemble of electrons in an ionized gas is

$$\frac{\partial f}{\partial t} + \boldsymbol{v} \cdot \nabla f - \frac{e}{m}\boldsymbol{E} \cdot \nabla_{\mathbf{v}} f = C[f], \tag{1}$$

where f is the electron distribution in six-dimensional phase space, $\boldsymbol{v}$ are the velocity coordinates, e is the elementary charge, m is the electron mass, $\boldsymbol{E}$ is the electric field, $\nabla_{\mathbf{v}}$ is the velocity-gradient operator and C represents the rate of change in f due to collisions.

To be able to solve the BE, we need to make drastic simplifications. To start with, we limit ourselves to the case where the electric field and the collision probabilities are all spatially uniform, at least on the scale of the collisional mean free path. The electron distribution f is then symmetric in velocity space around the electric field direction. In position space f may vary only along the field direction. Using spherical coordinates in velocity space, we obtain

$$\frac{\partial f}{\partial t} + v\cos\theta\frac{\partial f}{\partial z} - \frac{e}{m}E\left(\cos\theta\frac{\partial f}{\partial v} + \frac{\sin^2\theta}{v}\frac{\partial f}{\partial\cos\theta}\right) = C[f], \tag{2}$$

where v is the magnitude of the velocity, θ is the angle between the velocity and the field direction and z is the position along this direction.

The electron distribution f in equation (2) depends on four coordinates: v, θ, t and z. The next few sections describe how we deal with this. We simplify the θ-dependence by the classical two-term approximation (section 2.1). To simplify the time dependence, we only consider steady-state cases where the electric field and the electron distribution are either stationary or oscillate at high frequency (section 2.3). Additional exponential dependence of f on t or on z is assumed to account for electron production or loss due to ionization and attachment (section 2.2). We then describe the collision term (section 2.4), put all pieces together into one equation for the EEDF (section 2.5), and discuss the numerical techniques we use to solve this equation (section 2.6).

2.1. Two-term approximation

A common approach to solve equation (2) is to expand f in terms of Legendre polynomials of $\cos\theta$ (spherical harmonics expansion) and then construct from equation (2) a set of equations for the expansion coefficients. For high precision results six or more expansion terms are needed [15], but for many cases a two-term approximation already gives useful results. This two-term approximation is often used (e.g. by the BE solvers BOLSIG and ELENDIF) and has been extensively discussed in the literature [19, 20]. Although the approximation is known to fail for high values of E/N when most collisions are inelastic and f becomes strongly anisotropic [21], the errors in the calculated transport coefficients and rate coefficients are acceptable for fluid discharge modelling in the usual range of discharge conditions. Note that when the two-term approximation fails, some other, intrinsic approximations of fluid models also fail.

Using the two-term approximation we expand f as

$$f(v, \cos\theta, z, t) = f_0(v, z, t) + f_1(v, z, t)\cos\theta, \quad (3)$$

where f_0 is the isotropic part of f and f_1 is an anisotropic perturbation. Note that θ is defined with respect to the field direction, so f_1 is negative; this differs from some other texts where θ is defined with respect to the electron drift velocity and f_1 is positive. Also note that f is normalized as

$$\iiint f \,\mathrm{d}^3v = 4\pi \int_0^\infty f_0 v^2 \,\mathrm{d}v = n, \quad (4)$$

where n is the electron number density.

Equations for f_0 and f_1 are found from equation (2) by substituting equation (3), multiplying by the respective Legendre polynomials (1 and $\cos\theta$) and integrating over $\cos\theta$:

$$\frac{\partial f_0}{\partial t} + \frac{\gamma}{3}\varepsilon^{1/2}\frac{\partial f_1}{\partial z} - \frac{\gamma}{3}\varepsilon^{-1/2}\frac{\partial}{\partial \varepsilon}(\varepsilon E f_1) = C_0, \quad (5)$$

$$\frac{\partial f_1}{\partial t} + \gamma\varepsilon^{1/2}\frac{\partial f_0}{\partial z} - E\gamma\varepsilon^{1/2}\frac{\partial f_0}{\partial \varepsilon} = -N\sigma_\mathrm{m}\gamma\varepsilon^{1/2} f_1, \quad (6)$$

where $\gamma = (2e/m)^{1/2}$ is a constant and $\varepsilon = (v/\gamma)^2$ is the electron energy in electronvolts. The right-hand side of equation (5) represents the change in f_0 due to collisions and will be discussed in detail in section 2.4. The right-hand side of equation (6) contains the total momentum-transfer cross-section σ_m consisting of contributions from all possible collision processes k with gas particles:

$$\sigma_\mathrm{m} = \sum_k x_k \sigma_k, \quad (7)$$

where x_k is the mole fraction of the target species of the collision process; realize that the gas can be a mixture of different species, including excited states[1]. For elastic collisions, σ_k is the effective momentum-transfer cross-section, as clearly discussed in [22], accounting for possible anisotropy of the elastic scattering. For inelastic collisions, σ_k is the total cross section, assuming that all momentum is lost in the collision, i.e. that the remaining electron velocity after the collision is scattered isotropically. One needs to be careful about the definition of σ_m: omitting, for example, the contribution from inelastic collisions completely changes the calculation results; some data for σ_m in the literature are unclear on this point.

2.2. Growth of the electron density

We further simplify equations (5) and (6) by making assumptions about the temporal and spatial dependence of f_0 and f_1. In general f cannot be constant in both time and space because some collision processes (ionization, attachment) do not conserve the total number of electrons. Previous work [19, 22–24] proposed a simple technique to approximately describe the effects of net electron production in swarm type experiments. Following this technique, we separate the energy-dependence of f from its dependence on time and space by assuming that

$$f_{0,1}(\varepsilon, z, t) = \frac{1}{2\pi\gamma^3} F_{0,1}(\varepsilon) n(z, t), \quad (8)$$

where the energy distribution $F_{0,1}$ is constant in time and space and normalized by

$$\int_0^\infty \varepsilon^{1/2} F_0 \,\mathrm{d}\varepsilon = 1. \quad (9)$$

The time or space dependence of the electron density n is now related to the net electron production rate. For this, we consider two simple cases corresponding to specific swarm experiments. Most discharges resemble at least one of these cases.

Exponential temporal growth without space dependence. This case corresponds to Pulsed Townsend experiments [11]. The temporal growth rate of the electron number density equals the net production frequency $\bar{\nu}_i$:

$$\frac{1}{n_\mathrm{e}}\frac{\partial n_\mathrm{e}}{\partial t} = \bar{\nu}_i \equiv N\gamma \int_0^\infty \left(\sum_{k=\text{ionization}} x_k\sigma_k - \sum_{k=\text{attachment}} x_k\sigma_k \right) \times \varepsilon F_0 \,\mathrm{d}\varepsilon, \quad (10)$$

where the sum is over the ionization and attachment processes; we remind that x_k is the mole fraction of the target species of collision process k.

Equation (6) becomes

$$F_1 = \frac{E}{N}\frac{1}{\tilde{\sigma}_\mathrm{m}}\frac{\partial F_0}{\partial \varepsilon}, \quad (11)$$

where

$$\tilde{\sigma}_\mathrm{m} = \sigma_\mathrm{m} + \frac{\bar{\nu}_i}{N\gamma\varepsilon^{1/2}}. \quad (12)$$

Substituting this in equation (5), we find

$$-\frac{\gamma}{3}\frac{\partial}{\partial\varepsilon}\left(\left(\frac{E}{N}\right)^2 \frac{\varepsilon}{\tilde{\sigma}_\mathrm{m}}\frac{\partial F_0}{\partial\varepsilon}\right) = \tilde{C}_0 + \tilde{R}, \quad (13)$$

where the collision term

$$\tilde{C}_0 = 2\pi\gamma^3\varepsilon^{1/2}\frac{C_0}{Nn} \quad (14)$$

has been divided by the gas density N and the electron density n with respect to the collision term C_0 in equation (5), which makes it largely independent of these densities[2]. The term

$$\tilde{R} = -\frac{\bar{\nu}_i}{N}\varepsilon^{1/2} F_0 \quad (15)$$

ensures that F_0 remains normalized to unity in the case of net electron production. Previous work [23] interpreted this term as the energy needed to heat the secondary electrons up to the mean electron energy.

[1] The momentum-transfer cross-section σ_m appearing in equation (5) is equivalent to the diffusion cross section discussed in [22]. It can also be identified with the effective momentum-transfer cross-section derived from analysis of swarm experiments, at least at low E/N where ionization can be treated as an excitation process.

[2] Note that $\tilde{C}_0$ and C_0 are physical quantities and not collision operators as used in some other texts.

Exponential spatial growth without time dependence. This case corresponds to Steady State Townsend experiments [11]. While the electrons drift against the electric field their flux and density grow exponentially with a constant spatial growth rate α (Townsend coefficient), which is related to the net electron production by

$$\alpha \equiv -\frac{1}{n}\frac{\partial n}{\partial z} = -\frac{\bar{\nu}_i}{w}, \tag{16}$$

where the mean velocity w is determined by F_1, constant in space and negative.

Using the definition of α, equation (6) becomes

$$F_1 = \frac{1}{\sigma_m}\left(\frac{E}{N}\frac{\partial F_0}{\partial \varepsilon} + \frac{\alpha}{N}F_0\right) \tag{17}$$

and equation (5) can again be written in the form

$$-\frac{\gamma}{3}\frac{\partial}{\partial \varepsilon}\left(\left(\frac{E}{N}\right)^2 \frac{\varepsilon}{\tilde{\sigma}_m}\frac{\partial F_0}{\partial \varepsilon}\right) = \tilde{C}_0 + \tilde{R}, \tag{18}$$

where this time $\tilde{\sigma}_m = \sigma_m$ and the growth-renormalization term is

$$\tilde{R} = \frac{\alpha}{N}\frac{\gamma}{3}\left[\frac{\varepsilon}{\sigma_m}\left(2\frac{E}{N}\frac{\partial F_0}{\partial \varepsilon} + \frac{\alpha}{N}F_0\right) + \frac{E}{N}F_0\frac{\partial}{\partial \varepsilon}\left(\frac{\varepsilon}{\sigma_m}\right)\right]. \tag{19}$$

The value of α is found from combining equations (16) and (17):

$$w = \frac{1}{3}\gamma\int_0^\infty F_1 \varepsilon \,\mathrm{d}\varepsilon \equiv -\mu E + \alpha D = -\frac{\bar{\nu}_i}{\alpha}, \tag{20}$$

which yields

$$\alpha = \frac{1}{2D}(\mu E - \sqrt{(\mu E)^2 - 4D\bar{\nu}_i}), \tag{21}$$

where μ and D are written out and identified with the mobility and the diffusion coefficient, respectively, in section 3.1.

2.3. High frequency fields

The quasi-stationary approach of the previous sections assumes that the electric field remains constant on the time scale of the collisions. With some slight modifications, however, the same approach can also be used for high-frequency oscillating fields [19]. Using the complex notation, we express the oscillating electric field as

$$E(t) = E_0\,\mathrm{e}^{\mathrm{i}\omega t}. \tag{22}$$

Rather than equation (3), we use the following two-term approximation:

$$f(v, \cos\theta, z, t) = f_0(v, z, t) + f_1(v, z, t)\cos\theta\,\mathrm{e}^{\mathrm{i}\omega t}, \tag{23}$$

where the time-variation of f_0 and f_1 is slow with respect to the oscillation; f_1 may be complex to account for phase shifts with respect to the electric field.

Equation (23) is appropriate if the field frequency is so high that the electron energy lost over one field cycle is small. For elastic collisions this implies that the field frequency should be much greater than the collision frequency times the ratio of the electron mass to the gas particle mass: $\omega/N \gg (2m/M)\sigma_m\gamma\varepsilon^{1/2}$. A frequency limit related to inelastic collisions is more difficult to estimate. In practice equation (23) is reasonable for field frequencies in the gigahertz range (microwave discharges) and beyond (optical breakdown). For intermediate field frequencies, where the energy transfer per cycle is neither full nor negligible, a more complete solution of the time-dependent BE is necessary [25].

Using equation (23), we proceed exactly as before. Only the temporal growth model makes sense, because the high frequency field does not lead to time-averaged transport, and we find

$$F_1 = \frac{E_0}{N}\frac{\tilde{\sigma}_m - \mathrm{i}q}{\tilde{\sigma}_m^2 + q^2}\frac{\partial F_0}{\partial \varepsilon}, \tag{24}$$

where $\tilde{\sigma}_m = \sigma_m + \bar{\nu}_i/N\gamma\varepsilon^{1/2}$ and $q = \omega/N\gamma\varepsilon^{1/2}$. Substituting this in the equation for F_0 and averaging the energy absorption over the field cycle, we finally obtain

$$-\frac{\gamma}{3}\frac{\partial}{\partial \varepsilon}\left(\left(\frac{E_0}{N}\right)^2 \frac{\tilde{\sigma}_m \varepsilon}{2(\tilde{\sigma}_m^2 + q^2)}\frac{\partial F_0}{\partial \varepsilon}\right) = \tilde{C}_0 + \tilde{R}, \tag{25}$$

where the growth-renormalization term $\tilde{R}$ is given by equation (15).

We remark that in the case of a constant momentum-transfer frequency $\nu = \tilde{\sigma}_m N\gamma\varepsilon^{1/2}$ (σ_m is inversely proportional to $\varepsilon^{1/2}$), equation (25) can be written exactly as equation (13) for a stationary electric field, where the field E is replaced by an effective field $E_{\mathrm{eff}} = 2^{-1/2}(1 + \omega^2/\nu^2)^{-1/2}E_0$. This concept of effective field is used by some authors [26] to relate the EEDF and the electron properties in oscillating fields to those in dc fields.

2.4. Collision terms

The right-hand sides of equations (13), (18) and (25) contain the collision term consisting of contributions from all different collision processes k with neutral gas particles and from electron–electron collisions:

$$\tilde{C}_0 = \sum_k \tilde{C}_{0,k} + \tilde{C}_{0,e}. \tag{26}$$

Here we describe these contributions in detail.

Elastic collisions. The effect of elastic collisions can be described by [20]

$$\tilde{C}_{0,k=\mathrm{elastic}} = \gamma x_k \frac{2m}{M_k}\frac{\partial}{\partial \varepsilon}\left[\varepsilon^2\sigma_k\left(F_0 + \frac{k_B T}{e}\frac{\partial F_0}{\partial \varepsilon}\right)\right], \tag{27}$$

where M_k is the mass of the target particles and T is their temperature. The first term represents the kinetic energy lost to the target particles and the second term is the energy gained from the target particles assuming that these are Maxwellian; this term is important only at very low E/N.

Excitation/de-excitation. Excitation and de-excitation collisions cause a discrete energy loss or gain, continuously removing electrons from the energy distribution and reinserting them somewhere else [19]:

$$\tilde{C}_{0,k=\text{inelastic}} = -\gamma x_k[\varepsilon\sigma_k(\varepsilon)F_0(\varepsilon) - (\varepsilon+u_k)\sigma_k(\varepsilon+u_k)\,F_0(\varepsilon+u_k)], \tag{28}$$

where u_k is the threshold energy of the collision and is negative for de-excitation. The two terms are known, respectively, as the scattering-out and scattering-in terms; the scattering-in term clearly vanishes for $\varepsilon < -u_k$ in the case of de-excitation.

Ionization. The effect of ionization depends on how the remaining energy is shared by the two electrons after ionization. For some gases differential cross sections can be found for the energy sharing, which usually show that the energy is shared less equally as the remaining energy is large [27]. Here we consider only the two limiting cases of equal and zero energy sharing. In the case of equal energy sharing:

$$\tilde{C}_{0,k=\text{ionization}} = -\gamma x_k[\varepsilon\sigma_k(\varepsilon)F_0(\varepsilon) - 2(2\varepsilon+u_k)\sigma_k(2\varepsilon+u_k)F_0(2\varepsilon+u_k)], \tag{29}$$

where the factor 2 in the scattering-in term represents the secondary electrons being inserted at the same energy as the primary electrons. In case the primary electron takes all remaining energy (zero sharing)

$$\tilde{C}_{0,k=\text{ionization}} = -\gamma x_k[\varepsilon\sigma_k(\varepsilon)F_0(\varepsilon) - (\varepsilon+u_k)\sigma_k(\varepsilon+u_k)F_0(\varepsilon+u_k)] + \delta(\varepsilon)\gamma x_k\int_0^\infty u\sigma_k(u)F_0(u)\,\mathrm{d}u, \tag{30}$$

where δ is the Dirac delta-function. The last term denotes the secondary electrons, which are all inserted at zero energy.

Attachment. Attachment simply removes electrons from the energy distribution:

$$\tilde{C}_{0,k=\text{attachment}} = -\gamma x_k\varepsilon\sigma_k(\varepsilon)F_0(\varepsilon). \tag{31}$$

Electron–electron collisions. Previous work [9] gives the following expression for the collision term due to electron–electron collisions, assuming the electron distribution to be isotropic:

$$\tilde{C}_{0,e} = a\frac{n}{N}\left[3\varepsilon^{1/2}F_0^2 + 2\varepsilon^{3/2}\frac{\partial\psi}{\partial\varepsilon}\frac{\partial}{\partial\varepsilon}\left(\varepsilon^{1/2}\frac{\partial F_0}{\partial\varepsilon}\right) + \psi\frac{\partial F_0}{\partial\varepsilon}\right], \tag{32}$$

where

$$\psi = 3A_1 - \frac{A_2}{\varepsilon} + 2\varepsilon^{1/2}A_3, \tag{33}$$

$$A_1 = \int_0^\varepsilon u^{1/2}F_0(u)\,\mathrm{d}u, \tag{34}$$

$$A_2 = \int_0^\varepsilon u^{3/2}F_0(u)\,\mathrm{d}u, \tag{35}$$

$$A_3 = \int_\varepsilon^\infty F_0(u)\,\mathrm{d}u, \tag{36}$$

$$a = \frac{e^2\gamma}{24\pi\varepsilon_0^2}\ln\Lambda, \qquad \Lambda = \frac{12\pi(\varepsilon_0 k_\mathrm{B}T_\mathrm{e})^{3/2}}{e^3 n^{1/2}}, \qquad k_\mathrm{B}T_\mathrm{e} = \frac{2}{3}eA_2(\infty). \tag{37}$$

After some manipulation this becomes:

$$\tilde{C}_{0,e} = a\frac{n}{N}\frac{\partial}{\partial\varepsilon}\left[3A_1F_0 + 2(A_2+\varepsilon^{3/2}A_3)\frac{\partial F_0}{\partial\varepsilon}\right], \tag{38}$$

which expresses the electron–electron collision term as the divergence of the electron flux in energy space. The first term of the flux represents cooling by collisions with colder electrons (A_1 is the fraction of electrons below ε) and the second term is usually heating (diffusion to higher energies). For a Maxwellian distribution function the two terms cancel out, as can be readily seen by substituting $F_0 \propto \exp(-\varepsilon/\tau)$ for arbitrary τ.

2.5. Equation for the EEDF

When combining the previous equations, we find an equation for F_0 that looks like a convection-diffusion continuity-equation in energy space:

$$\frac{\partial}{\partial\varepsilon}\left(\tilde{W}F_0 - \tilde{D}\frac{\partial F_0}{\partial\varepsilon}\right) = \tilde{S}, \tag{39}$$

where

$$\tilde{W} = -\gamma\varepsilon^2\sigma_\varepsilon - 3a\frac{n}{N}A_1, \tag{40}$$

$$\tilde{D} = \frac{\gamma}{3}\left(\frac{E}{N}\right)^2\frac{\varepsilon}{\tilde{\sigma}_\mathrm{m}} + \frac{\gamma k_\mathrm{B}T}{e}\varepsilon^2\sigma_\varepsilon + 2a\frac{n}{N}(A_2+\varepsilon^{3/2}A_3), \tag{41}$$

$$\sigma_\varepsilon = \sum_{k=\text{elastic}}\frac{2m}{M_k}x_k\sigma_k, \tag{42}$$

$$\tilde{S} = \sum_{k=\text{inelastic}}\tilde{C}_{0,k} + G. \tag{43}$$

It is instructive to interpret the left-hand side of equation (39) as the divergence of the electron flux in energy space. This flux then has a convection part with a negative flow velocity $\tilde{W}$, representing cooling by elastic collisions with less energetic particles (neutrals or electrons), and a diffusive part with diffusion coefficient $\tilde{D}$, representing heating by the field and by elastic collisions with more energetic particles. Note that in the case of HF fields the heating term is modified as discussed in section 2.3. Note also that the source term $\tilde{S}$ on the right-hand side of equation (39) has the special property that it is non-local: due to the scattering-in terms it depends on energies elsewhere in energy space. This means that the equation is no ordinary differential equation and solving it requires some special care.

2.6. Numerical solution of the equation

Equation (39) is discretized on a grid in energy space, consisting of a series of subsequent energy intervals, here called grid cells, numbered $i = 1, 2, \ldots$. The subscript i refers to the centre of the grid cell i and the subscript $i+\frac{1}{2}$ to the boundary between the cells i and $i+1$. The energy distribution function F_0 is defined in the cell centres. For each cell i we obtain a linear equation relating the local value $F_{0,i}$ to the values $F_{0,j}$ in the other cells, by integrating the differential equation over the cell:

$$\left[\tilde{W}F_0 - \tilde{D}\frac{\partial F_0}{\partial\varepsilon}\right]_{i+1/2} - \left[\tilde{W}F_0 - \tilde{D}\frac{\partial F_0}{\partial\varepsilon}\right]_{i-1/2} = \int_{\varepsilon_{i-1/2}}^{\varepsilon_{i+1/2}}\tilde{S}\,\mathrm{d}\varepsilon \tag{44}$$

and then discretizing the various terms.

The left-hand side of the equation is discretized by the exponential scheme of Scharfetter and Gummel [28] commonly used for convection-diffusion problems:

$$\left[\tilde{W}F_0 - \tilde{D}\frac{\partial F_0}{\partial \varepsilon}\right]_{i+1/2} = \frac{\tilde{W}_{i+1/2}F_{0,i}}{1-\exp[-z_{i+1/2}]} + \frac{\tilde{W}_{i+1/2}F_{0,i+1}}{1-\exp[z_{i+1/2}]}, \tag{45}$$

where $z_{i+1/2} = \tilde{W}_{i+1/2}(\varepsilon_{i+1}-\varepsilon_i)/\tilde{D}_{i+1/2}$ (Peclet number). This scheme is very accurate when the convection and diffusion terms are about equal, i.e. when inelastic collisions play no important role, and becomes equivalent to a second-order accurate central-difference scheme when the diffusion term is dominant. The electron–electron collision terms in $\tilde{W}$ and $\tilde{D}$ depend on F_0 and require iteration. To speed up convergence these terms are implicitly corrected. In addition, we start the iteration procedure from a Maxwellian distribution function at a temperature deduced from the global energy balance of the electrons.

The inelastic collision terms on the right-hand side are non-local in energy but linear in F_0 and are evaluated fully implicitly, which involves direct inversion of a matrix that is more or less sparse, depending on the different threshold energies of the collisions. We discretize as follows:

$$\int_{\varepsilon_{i-1/2}}^{\varepsilon_{i+1/2}} \tilde{S}\,\mathrm{d}\varepsilon \equiv -P_i F_{0,i} + \sum_j Q_{i,j}F_{0,j}, \tag{46}$$

where the two terms represent scattering-out and scattering-in:

$$P_i = \sum_{\text{inelastic}} \gamma x_k \int_{\varepsilon_{i-1/2}}^{\varepsilon_{i+1/2}} \varepsilon\sigma_k \exp[(\varepsilon_i-\varepsilon)g_i]\,\mathrm{d}\varepsilon, \tag{47}$$

$$Q_{i,j} = \sum_{\text{inelastic}} \gamma x_k \int_{\varepsilon_1}^{\varepsilon_2} \varepsilon\sigma_k \exp[(\varepsilon_j-\varepsilon)g_j]\,\mathrm{d}\varepsilon, \tag{48}$$

where the interval $[\varepsilon_1, \varepsilon_2]$ is the overlap of cell j, and cell i shifted by the threshold energy u_k:

$$\varepsilon_1 = \min(\max(\varepsilon_{i-1/2}+u_k, \varepsilon_{j-1/2}), \varepsilon_{j+1/2}), \tag{49}$$

$$\varepsilon_2 = \min(\max(\varepsilon_{i+1/2}+u_k, \varepsilon_{j-1/2}), \varepsilon_{j+1/2}). \tag{50}$$

The exponential factors in the P- and Q-integrals assume the distribution F_0 to be piecewise exponential, with a (local) logarithmic slope estimated as

$$g_i = \frac{1}{\varepsilon_{i+1}-\varepsilon_{i-1}} \ln\left(\frac{F_{0,i+1}}{F_{0,i-1}}\right). \tag{51}$$

This technique requires iteration but converges extremely rapidly. The P- and Q-integrals are calculated exactly, assuming the cross sections to be linear in between the points specified by the user in a table of cross section versus energy.

For simplicity we have not written out the effects of ionization or attachment in the above equations. In the case of ionization the scattering-in term accounts for the secondary electrons, as discussed before, and in the case of attachment there is no scattering-in. In either case an additional growth-renormalization term is included accounting for temporal or spatial growth, as discussed before. The growth-renormalization term is non-linear in F_0 and also requires iteration. To ensure convergence, however, this term must be linearized and partly evaluated implicitly. We use different ways of linearizing this term depending on the growth type (temporal growth or spatial growth) and on the sign of the net electron production (production or loss). We impose that the term integrated over all energies equals exactly the net production.

We impose the boundary condition that there is no flux in energy space at zero energy. In addition we impose the normalization condition.

3. Coefficients for fluid equations

Although more flexible than BOLSIG and most other solvers, our BE solver only describes the simplest discharge conditions: uniform electric field, uniform or exponentially growing electron density, etc. We now want to use the results from the BE solver to obtain transport coefficients and rate coefficient for fluid models which describe much more general conditions: arbitrarily varying electric fields, electron densities, etc. This implies a generalization of the coefficients as a function of E/N or mean electron energy, which is difficult to justify and should be seen as just an assumption made out of technical necessity. However, if we are careful about the definition of the coefficients, we can ensure that whenever the fluid model is used for the simple conditions assumed by the BE solver, it yields exactly the same mean velocity and mean energy as the solver. We thus obtain maximum consistency between the fluid model and the BE.

In order to find out how best to calculate the transport coefficients and rate coefficients from the energy distribution function F_0, we need to make the link between the two-term formulation of the BE equation, represented by equations (5) and (6), and the fluid equations. In the next few sections we discuss this for common fluid equations and their coefficients.

3.1. Electron transport

The continuity equation for electrons can be obtained from equation (5) by multiplying by $\varepsilon^{1/2}$ and integrating over all energies:

$$\frac{\partial n}{\partial t} + \frac{\partial \Gamma}{\partial z} = S, \tag{52}$$

where S is the net electron source term and the electron flux is

$$\Gamma = nw = n\frac{\gamma}{3}\int_0^\infty \varepsilon F_1\,\mathrm{d}\varepsilon. \tag{53}$$

Combining this with equation (6), we find the well-known drift-diffusion equation

$$\Gamma = -\mu E n - \frac{\partial(Dn)}{\partial z}, \tag{54}$$

where the mobility and diffusion coefficient are given by

$$\mu N = -\frac{\gamma}{3}\int_0^\infty \frac{\varepsilon}{\tilde{\sigma}_\mathrm{m}}\frac{\partial F_0}{\partial \varepsilon}\mathrm{d}\varepsilon, \tag{55}$$

$$DN = \frac{\gamma}{3}\int_0^\infty \frac{\varepsilon}{\tilde{\sigma}_\mathrm{m}} F_0\,\mathrm{d}\varepsilon. \tag{56}$$

The effective momentum-transfer cross-section $\tilde{\sigma}_\mathrm{m}$ in these equations includes the effect of possible temporal growth as

given by equation (12). Although the normalized energy distribution F_0 is assumed to be independent of space when solving the BE, the above fluid equations and coefficient definitions are also valid in case the energy distribution is space dependent. The diffusion coefficient in equation (54) then clearly appears inside the divergence and can generally not be put in front of it, as is done in Fick's law.

3.2. Energy transport

Similar to the derivation of the continuity equation in the previous section, the energy equation is obtained from equation (5) by multiplying by $\varepsilon^{3/2}$ and integrating:

$$\frac{\partial n_\varepsilon}{\partial t} + \frac{\partial \Gamma_\varepsilon}{\partial z} + E\Gamma = S_\varepsilon, \tag{57}$$

where the energy density and the energy flux are given by

$$n_\varepsilon = n\int_0^\infty \varepsilon^{3/2} F_0 \,\mathrm{d}\varepsilon \equiv n\bar{\varepsilon}, \tag{58}$$

$$\Gamma_\varepsilon = n\frac{\gamma}{3}\int_0^\infty \varepsilon^2 F_1 \,\mathrm{d}\varepsilon, \tag{59}$$

where $\bar{\varepsilon}$ is the mean electron energy in electronvolts. The last term on the left-hand side of equation (57) represents heating by the electric field; the term S_ε on the right-hand side is the total energy transfer (usually loss) due to collisions. Using equation (6), we can write the energy flux as well in a drift-diffusion form:

$$\Gamma_\varepsilon = -\mu_\varepsilon E n_\varepsilon - \frac{\partial(D_\varepsilon n_\varepsilon)}{\partial z}, \tag{60}$$

where the energy mobility and the energy diffusion coefficient are defined by

$$\mu_\varepsilon N = -\frac{\gamma}{3\bar{\varepsilon}}\int_0^\infty \frac{\varepsilon^2}{\tilde{\sigma}_\mathrm{m}}\frac{\partial F_0}{\partial \varepsilon}\,\mathrm{d}\varepsilon, \tag{61}$$

$$D_\varepsilon N = \frac{\gamma}{3\bar{\varepsilon}}\int_0^\infty \frac{\varepsilon^2}{\tilde{\sigma}_\mathrm{m}} F_0 \,\mathrm{d}\varepsilon. \tag{62}$$

The above formulation of the energy equation is somewhat unusual but we recommend it because of its consistency with the two-term BE. The formulation is basically equivalent to that of Allis [29]; our energy mobility and diffusion coefficient are straightforwardly related to Allis' thermoelectricity β and heat diffusion G as $\mu_\varepsilon = \beta/\bar{\varepsilon}$ and $D_\varepsilon = G/\bar{\varepsilon}$; some other authors using this approach are Ingold [30] and Alves *et al* [31].

Other formulations of the energy equation found in the literature [32] show a separation of the electron energy flux into a convective part proportional to the electron flux and a thermal conduction part proportional to the gradient of the mean electron energy; this however involves additional assumptions and may lead to ambiguity in the definition of the energy transport coefficients (e.g. the thermal conductivity appearing in such energy equations); some further discussion on this issue is given in section 4.5.

Note also that the above formulation of the energy equation is technically convenient because it has exactly the same form as the particle continuity equation and can be solved for n_ε by the same numerical routine. The mean energy is subsequently obtained by dividing, $\bar{\varepsilon} = n_\varepsilon/n$. A semi-implicit technique to avoid numerical instabilities due to the possible energy-dependence of the source term S_ε has previously been developed [33] and proved to work very well.

3.3. Source terms

Various coefficients can be defined for the purpose of calculating the reaction rates appearing in the source terms of fluid equations. Most straightforward is to define rate coefficients (in units of volume per time) as

$$k_k = \gamma\int_0^\infty \varepsilon\sigma_k F_0 \,\mathrm{d}\varepsilon, \tag{63}$$

from which the reaction rate for the collision processes k is obtained by multiplication by the density of the electrons and the target species:

$$R_k = k_k x_k N n. \tag{64}$$

In an alternative approach one can define Townsend coefficients α_k (in units of inverse length) such that

$$R_k = \alpha_k x_k |\Gamma|. \tag{65}$$

For the cases of temporal and spatial growth discussed in section 2.2, these Townsend coefficients are then given by

$$\frac{\alpha_k}{N} = \frac{k_k \alpha}{\bar{\nu}_i} \tag{66}$$

and

$$\frac{\alpha_k}{N} = \frac{k_k}{\mu E}. \tag{67}$$

Using Townsend coefficients, the reaction rates are calculated from the electron flux rather than from the electron density. Clearly this makes no difference for the cases of pure spatial or temporal growth, but in general equations (66) and (67) yield different results. It is recommended to use rate coefficients in situations where the electrons diffuse against the electric force (plasma bulk) and Townsend coefficients in situations where the flux is field driven. The use of Townsend coefficients is especially recommended for modelling the cathode region in dc discharges, where the poor physical reality of the drift-diffusion equation leads to large errors in the electron density but hardly affects the electron flux; models without energy equation may not even have a solution when rate coefficients are used in the cathode fall.

3.4. High frequency momentum equation

Some models of HF discharges use an electron momentum equation of the form

$$\frac{\partial w}{\partial t} + \bar{\nu}_\mathrm{eff} w = -\phi\frac{e}{m}E, \tag{68}$$

where w is the electron drift velocity and $\bar{\nu}_\mathrm{eff}$ is an effective collision frequency. The factor ϕ is usually omitted, but we show here that this factor is needed to be consistent with the BE. According to the two-term approach of section 2.3, and using the complex notation, the electron drift velocity in HF fields is equal to

$$\begin{aligned} w &= \gamma \mathrm{e}^{\mathrm{i}\omega t}\int_0^\infty \varepsilon F_1 \,\mathrm{d}\varepsilon = -\frac{\gamma E}{3N}\int_0^\infty \varepsilon\frac{\tilde{\sigma}_\mathrm{m} - \mathrm{i}q}{\tilde{\sigma}_\mathrm{m}^2 + q^2}\frac{\partial F_0}{\partial \varepsilon}\mathrm{d}\varepsilon \\ &\equiv -(\mu_r + \mathrm{i}\mu_i)E, \end{aligned} \tag{69}$$

which defines a complex electron mobility $\mu = \mu_r + \mathrm{i}\mu_i$. Substituting this in the momentum equation, we find that the coefficients must be calculated as

$$\bar{\nu}_{\mathrm{eff}} = -\frac{\mu_r}{\mu_i}\omega, \tag{70}$$

$$\phi = -\frac{\mu_r^2 + \mu_i^2}{\mu_i}\frac{m_e\omega}{e}. \tag{71}$$

The factor ϕ equals unity for a constant momentum-transfer frequency (σ_m inversely proportional to $\varepsilon^{1/2}$) but may be quite different from unity in case the momentum-transfer frequency depends on energy. This has been pointed out previously [34] but is frequently overlooked.

We remark that, strictly speaking, the momentum equation (68) is not very useful to describe the electron motion in a pure harmonic HF field, since the electron drift velocity w can be obtained directly from the complex mobility by equation (69). However, the momentum equation is useful to describe more general cases where the electric field is not purely harmonic, but resembles a harmonic oscillation at a certain frequency.

4. Examples of results

We have extensively tested our BE solver for the gases argon and nitrogen. These are model gases used in many BE calculations described in the literature; we use the cross sections recommended by Phelps [35]. As default options for our calculations we consider the assumptions done by BOLSIG and most other BE solvers available: exponential temporal growth, quasi-stationary electric field, only collisions with ground state gas particles. For these assumptions our calculation results are identical to those obtained with BOLSIG. We consider that this exact agreement obtained using two very different solution techniques validates each. The typical calculation time for one EEDF is on the order of a few tens of milliseconds on a standard 2 GHz PC.

Calculation results for the default options are so well known from previous work that there is no use showing them again in this paper. Instead, we show results for options different from default, not included in BOLSIG and most other solvers. The next few sections illustrate the influence of the growth model (section 4.1), electron–electron collisions (section 4.2), electron collisions with excited neutrals (section 4.3), high frequency field oscillations (section 4.4), and some commonly used assumptions concerning the transport coefficients (section 4.5). Similar results have been presented previously and are known to BE specialists, but often overlooked by developers and users of fluid models. Our aim here is to provide a feeling of how and when the new options of our BE solver should be used and how they might affect the fluid model coefficients. We do not intend to be exhaustive; the presented results are just illustrative examples and more systematic investigation is saved for future work.

4.1. Influence of growth model

When solving the BE one needs to make assumptions on what happens if collision processes (ionization, attachment) do not conserve the total number of electrons. In section 2.2 we discussed two model cases included in our BE solver, where the net production (loss) of electrons leads to exponential temporal growth (decay) and exponential spatial growth (decay) of the electron density. Clearly these are only ideal cases that do not always exactly fit real discharges. Some discharges, such as a fully developed dc glow discharge between parallel plates, closely resemble the case of exponential spatial growth. Other discharge situations, such as the ignition of a dielectric barrier discharge, have features of both spatial and temporal growth. Yet other discharge situations cannot be described by either of the exponential growth models; in a dc positive column, for example, net production is balanced by transverse diffusion loss. There is no growth model that works for all discharges, but we estimate that for many cases the exponential spatial growth model is probably the most realistic. Note however that BOLSIG and most other solvers assume exponential temporal growth.

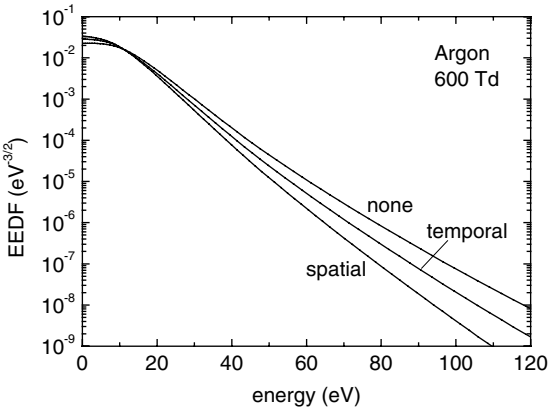

Figure 1. EEDF for 600 Td in argon calculated using the exponential temporal growth model, exponential spatial growth model, and neglecting growth (treating ionization as excitation).

In general the growth effects reduce the mean electron energy (for a given E/N) but have only a minor influence on the shape of the EEDF (for a given mean energy). This is illustrated for argon by figure 1, which compares the EEDFs for the different exponential growth models with the EEDF when growth is neglected, i.e. when ionization is treated as an excitation process and no secondary electrons are inserted. Note that the difference between the two exponential growth models is on the same order as the difference between the temporal growth model and no growth model at all. Figure 2 then shows the influence of the growth effects on the ionization rate coefficient in argon. Although the differences between the curves for the different growth models in figure 2 seem relatively small, our experience is that they can have serious consequences for the fluid simulation results. More systematic investigation on this point is definitely needed but beyond the scope of this paper.

4.2. Influence of electron–electron collisions

Electron–electron collisions cause the EEDF to tend towards a Maxwellian distribution function. The influence of these collisions depends essentially on the ionization degree n/N and is known to become significant for $n/N > 10^{-6}$ in some gases. Note from equation (32) that there is also a

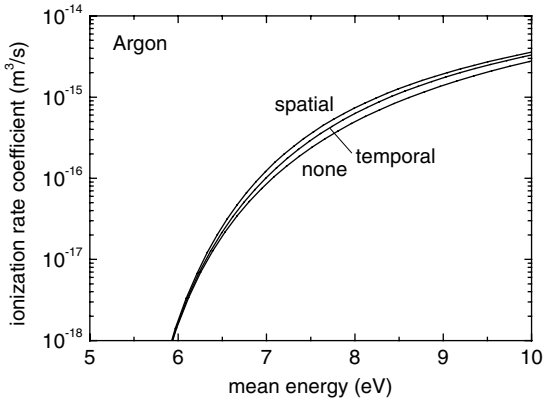

Figure 2. Ionization rate coefficient in argon for different exponential growth models.

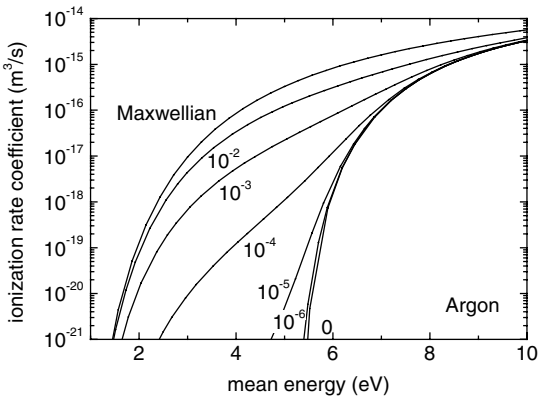

Figure 4. Ionization rate coefficient in argon, taking into account electron-electron collisions, for different ionization degrees and for a Maxwellian EEDF.

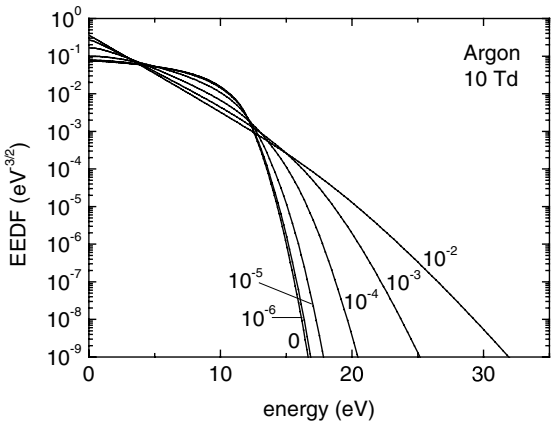

Figure 3. EEDF for 10 Td in argon, taking into account electron–electron collisions, for different ionization degrees.

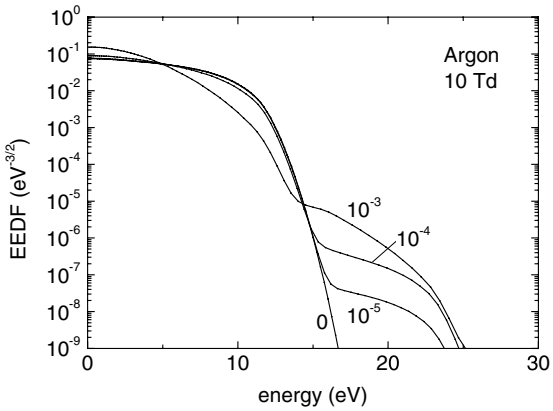

Figure 5. EEDF for 10 Td in argon, taking into account collisions with excited neutrals, for different excitation degrees.

weak dependence on the plasma density which appears in the Coulomb logarithm accounting for the screening of the Coulomb potential by space charge effects. Figure 3 shows the EEDF in argon for different ionization degrees, a plasma density of 10^{18} m^{-3} and a weak reduced electric field of 10 Td. For increasing ionization degree the EEDF resembles more and more a Maxwellian distribution function, i.e. a straight line in the logarithmic plot of figure 3.

These effects are usually neglected in fluid models, but is this justified? The most important consequence of electron–electron collisions for fluid models is that they increase the rate coefficients of inelastic collisions (ionization, excitation) by repopulating the tail of the EEDF. This is illustrated by figure 4 which shows the ionization rate coefficient of ground state argon for different ionization degrees. The inelastic rate coefficients may be strongly increased for ionization degrees of 10^{-5} and higher, but only at low mean electron energy, because the cross-section for electron–electron collisions drops off rapidly with increasing electron energy.

The eventual consequences of this for fluid simulations clearly depend on the discharge conditions. Many discharges have such low ionization degree or such high mean electron energy that it is perfectly justified to neglect the influence of electron–electron collisions. Some discharges, however, operate at precisely those conditions where electron–electron collisions are important; microwave discharges, for example, can have a high ionization degree beyond 10^{-5} and a low electron mean energy of only a few electronvolts. These conditions occur typically in discharges sustained by stepwise ionization and where the EEDF is also influenced by electron collisions with excited neutrals; see section 4.3.

We remark that it may be technically cumbersome to account for the influence of electron–electron collisions in a fluid model: due to these collisions the rate coefficients are functions not only of E/N or the mean energy, but also of the ionization degree n/N; this implies using two-dimensional interpolation tables.

4.3. Influence of collisions with excited neutrals

Collisions with excited neutrals may be super-elastic and accelerate electrons immediately into the tail of the EEDF. The influence of this on the EEDF is shown by figure 5 for argon for different excitation degrees (fractional densities of excited neutrals). The results in this figure have been obtained by regrouping all excited argon states in one compound state, for which we estimated an overall super-elastic cross-section by detailed balancing, taking into account only transitions to the ground state.

As with electron–electron collisions, the most important consequence for fluid simulations is an increase of the rate

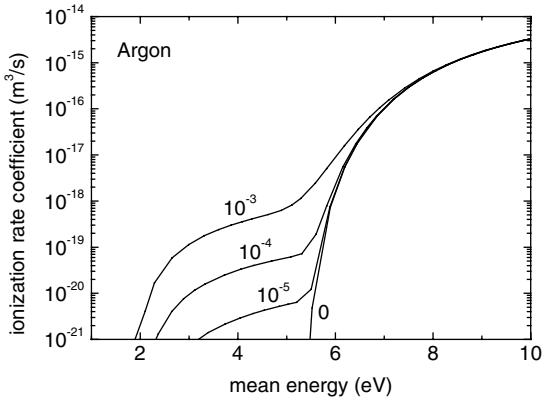

Figure 6. Ionization rate coefficient in argon, taking into account collisions with excited neutrals, for different excitation degrees.

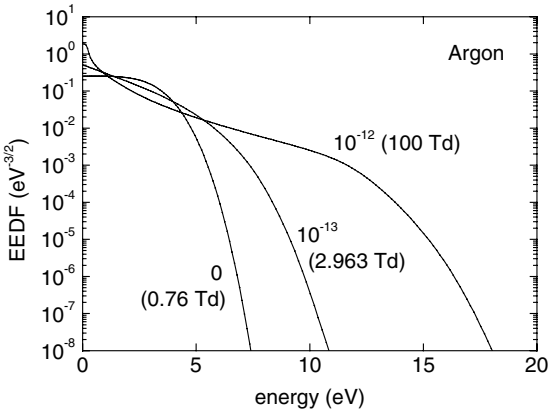

Figure 7. EEDF in argon for oscillating electric fields with different amplitudes and different reduced frequencies ω/N (in units of $\mathrm{m^3\,s^{-1}}$), each having the same mean electron energy of 2.150 eV.

coefficients of inelastic collisions at low mean electron energy. Figure 6 shows the ionization rate coefficient of ground state argon. See further our discussion on electron–electron collisions.

4.4. Influence of high-frequency oscillations

In HF oscillating fields with a frequency comparable with or greater than the collision frequency, the electron heating is less efficient than in dc fields. As a result, a stronger reduced field is required to achieve the same mean electron energy. In addition the shape of the EEDF may be different (for the same mean energy), because the electron heating depends differently on collisional momentum transfer: in dc fields collisions impede the heating whereas in HF fields they enhance it; compare the electron heating terms in equations (13) and (25). In gases where the momentum-transfer frequency depends strongly on the electron energy, this leads to large differences in the shape of EEDF. This is illustrated by figure 7, which shows the EEDF in argon for the same mean energy and for different reduced field-frequencies ω/N.

Rate coefficients for fluid models of HF discharges (e.g. microwave discharges) need to account for the field-oscillation effects on the shape of the EEDF. Figure 8 shows the ionization rate coefficient of ground state argon as a function of the

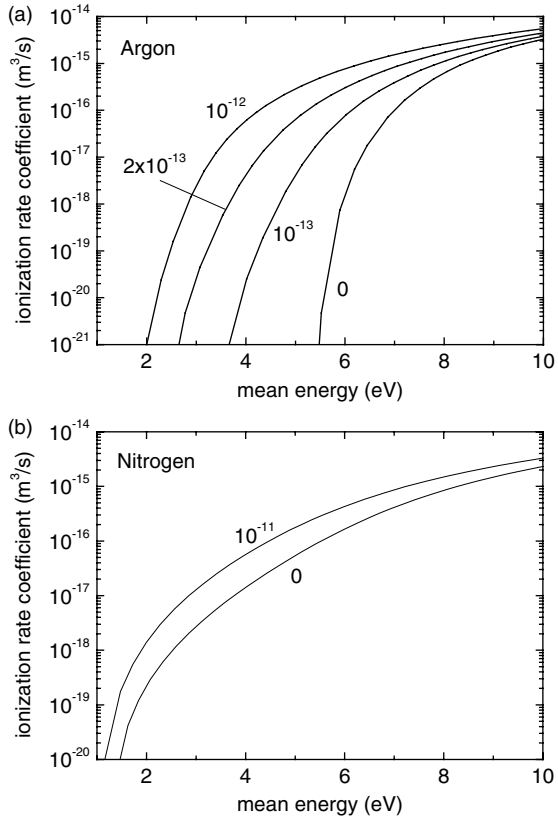

Figure 8. Ionization coefficient in (*a*) argon and (*b*) nitrogen for oscillating electric fields with different reduced frequencies ω/N (in units of $\mathrm{m^3\,s^{-1}}$).

mean energy for different reduced frequencies. The effects are important mainly at lower mean electron energy (where more electrons see the Ramsauer minimum in the elastic collision cross section) which is exactly where most HF discharges operate. The influence of the oscillations is much less important in gases with a more constant collision frequency, as is illustrated in figure 8 for the case of nitrogen.

When implementing the high-frequency rate coefficients in a fluid model a technical complication can arise when the gas is heated by the discharge such that ω/N is not constant; two-dimensional interpolation tables may then be necessary. We also remark that for some gases and some values of ω/N the mean energy may not be a monotonic function of E/N: there may exist two different EEDFs with the same mean energy, so that it becomes impossible to define rate coefficients or transport coefficients as unique functions of the mean energy. We found this behaviour for argon for a wide range of ω/N (10^{-13}–$10^{-11}\,\mathrm{m^3\,s^{-1}}$) and low mean energies (around 2 eV), but not for nitrogen.

4.5. Accuracy of some common approximations

Fluid models often use approximations concerning the transport coefficients, such as the Einstein relation between the diffusion coefficient and the mobility. In this section we check some of these approximations against the results of our BE solver in order to get an idea of their accuracy.

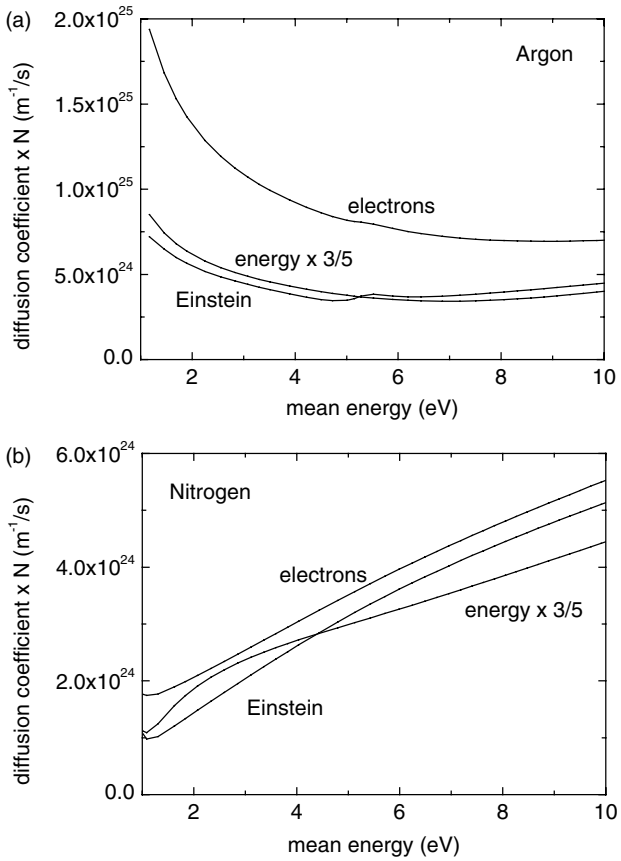

Figure 9. Diffusion coefficients in (*a*) argon and (*b*) nitrogen for electrons and electron energy, calculated precisely and calculated from the Einstein relation.

The commonly used Einstein relation is [36]:

$$D = \tfrac{2}{3}\mu\bar{\varepsilon}, \tag{72}$$

which is exact for a Maxwellian EEDF or a constant momentum-transfer frequency (σ_m inversely proportional to $\varepsilon^{1/2}$) but more or less approximate for real discharge situations. To illustrate the possible errors of the Einstein relation, figure 9 shows the diffusion coefficient in argon and in nitrogen calculated exactly from equation (62) and calculated from the Einstein relation. For argon the Einstein relation is off by a factor 2 due to the strong energy-dependence of the momentum-transfer frequency; for nitrogen the errors are much smaller.

One must realize, however, that the results of our BE solver are approximations as well. For instance, more detailed analysis [37] shows different diffusion coefficients for transport along and perpendicular to the electric field direction, whereas this distinction vanishes with our BE solver based on the two-term expansion. Realize also that for many discharge conditions the drift-diffusion equation itself gives a rather bad description of reality, without this having too serious consequences for the discharge simulation as a whole [38]. In the cathode region of dc discharges the drift-diffusion equation is known to lead to large errors in the electron density without seriously affecting the rest of the discharge; also see our also remarks in section 3.3.

Further common approximations concern the electron energy transport. Many fluid models in the literature use an electron energy equation where (once written as equation (60)) the energy transport coefficients are given by

$$\mu_\varepsilon = \tfrac{5}{3}\mu \qquad \text{and} \qquad D_\varepsilon = \tfrac{5}{3}D. \tag{73}$$

These approximations can be derived by assuming a Maxwellian EEDF, a constant momentum-transfer frequency and constant kinetic pressure [36]. The approximations allow the separation of the energy flux into a part proportional to the electron flux and a part proportional to the gradient of the mean energy, as in classical fluid mechanics:

$$\Gamma_\varepsilon = \tfrac{5}{3}\Gamma\bar{\varepsilon} - \tfrac{5}{3}nD\nabla\bar{\varepsilon}, \tag{74}$$

where the factor in front of the energy gradient is the electron thermal conductivity.

Some authors [29–31] however avoid the approximations given by equation (73) and calculate the energy transport coefficients more precisely as discussed in section 3.2. To illustrate the difference between the approximations and the more precise expressions given by equations (61) and (62), figure 9 also shows the energy diffusion coefficient D_ε calculated from equation (62) and multiplied by 3/5, which (according to equation (73)) is to be compared with the electron diffusion coefficient D. Once again the difference is about a factor 2 for argon and much smaller for nitrogen. For the energy mobility μ_ε the difference is usually much smaller than for D_ε. To our knowledge the consequences of equation (73) for fluid simulations have never been investigated systematically, but one can imagine that for some gases they are quite significant.

5. Conclusions

We have developed a new user-friendly BE solver to calculate the electron transport coefficients and rate coefficients that are input data for fluid models. Our BE solver is called the BOLSIG+ and is available as a freeware [18]. The solver provides steady-state solutions of the BE for electrons in a uniform electric field, using the classical two-term expansion, and is able to account for different growth models, quasi-stationary and oscillating fields, electron–neutral collisions and electron–electron collisions. We show that for the approximations we use, the BE takes the form of a convection-diffusion continuity-equation with a non-local source term. To solve this equation we use an exponential scheme commonly used for convection-diffusion problems. The calculation time for one EEDF is on the order of tens of milliseconds on a standard 2 GHz PC. The calculated electron coefficients are defined so as to ensure maximum consistency with the fluid equations. Special care must be taken of the transport coefficients for electron energy, for which we recommend the formulation proposed previously by Allis [29].

We have illustrated the influence of several non-standard options included in our BE solver, frequently overlooked by users and developers of fluid models. The results from our BE solver show that growth effects significantly reduce the mean electron energy and the ionization rate coefficient; there are also significant differences between the exponential models for temporal and spatial growth. Electron–electron collisions may strongly increase the rate coefficients of

inelastic collisions (excitation, ionization) for low electron mean energies ($\ll$ threshold energy) and ionization degrees of 10^{-5} and higher; these conditions are present in some common gas discharges. A similar increase in the inelastic rate coefficients can be due to super-elastic collisions with excited neutrals for excitation degrees of 10^{-5} and higher. In HF oscillating fields the shape of the EEDF can be strongly modified by oscillation effects, causing large differences in the electron coefficients as a function of mean electron energy with respect to dc fields, especially for gases where the momentum-transfer frequency depends strongly on energy. For such gases also the Einstein relation can be wrong by as much as a factor 2, and special care must be taken about the definition of energy transport coefficients. All results presented here are just illustrative examples; more systematic investigation is necessary to obtain a complete picture of when and how best to use the different options of our BE solver.

References

[1] Ingold J H 1989 *Phys. Rev.* A **40** 3855–63
[2] Graves D B and Jensen K F 1986 *IEEE Trans. Plasma Sci.* **PS-14** 78
[3] Boeuf J-P 1987 *Phys. Rev.* A **36** 2782
[4] Salabas A, Gousset G and Alves L L 2002 *Plasma Sources Sci. Technol.* **11** 448
[5] Dutton J 1975 *J. Phys. Chem. Ref. Data* **4** 577
[6] Frost L S and Phelps A V 1962 *Phys. Rev.* **127** 1621
[7] Wilhelm R and Winkler R 1969 *Ann. Phys.* **23** 28
[8] Winkler R *et al* 1984 *Beitr. Plasmaphys.* **24** 657–74
[9] Rockwood S D 1973 *Phys. Rev.* A **40** 399
[10] Luft P E 1975 *JILA Information Center Report* No. 14 University of Colorado, Boulder
[11] Tagashira H, Sakai Y and Sakamoto S 1977 *J. Phys. D: Appl. Phys.* **10** 1051–63
[12] Morgan W L 1979 *JILA Information Center Report* No. 19 University of Colorado, Boulder
[13] Morgan W L and Penetrante B M 1990 *Comput. Phys. Commun.* **58** 127–52
[14] Lin S L, Robson R E and Mason E A 1979 *J. Chem. Phys.* **71** 3483–98
[15] Pitchford L C, ONeil S V and Rumble J J R 1981 *Phys. Rev.* A **23** 294
[16] Segur P *et al* 1983 *J. Comput. Phys.* **50** 116
[17] BOLSIG 1997 CPAT: http://www.cpat.ups-tlse.fr/operations/operation_03/POSTERS/BOLSIG/index.html
[18] BOLSIG+ 2005 CPAT: http://www.codiciel.fr/plateforme/plasma/bolsig/bolsig.php
[19] Holstein T 1946 *Phys. Rev.* **70** 367
[20] Allis W P 1956 *Handbuch der Physik* ed S Flugge (Berlin: Springer) p 383
[21] Allis W P 1982 *Phys. Rev.* A **26** 1704–12
[22] Phelps A V and Pitchford L C 1985 *Phys. Rev.* A **31** 2932–49
[23] Thomas W R L 1969 *J. Phys. B: At. Mol. Opt. Phys.* **2** 551
[24] Brunet H and Vincent P 1979 *J. Appl. Phys.* **50** 4700
[25] Wilhelm J and Winkler R 1979 *J. Phys.* **40** C7-251
[26] McDonald A D 1953 *Microwave Breakdown in Gases* (London: Oxford University Press)
[27] Opal C B, Peterson W K and Beaty E C 1971 *J. Chem. Phys.* **55** 4100
[28] Scharfetter D L and Gummel H K 1969 *IEEE Trans. Electron. Devices* **16** 64
[29] Allis W P 1967 *Electrons, Ions, and Waves* (Cambridge: MIT Press)
[30] Ingold J H 1997 *Phys. Rev.* E **56** 5932–44
[31] Alves L L, Gousset G and Ferreira C M 1997 *Phys. Rev.* E **55** 890–906
[32] Boeuf J P and Pitchford L C 1995 *Phys. Rev.* E **51** 1376–90
[33] Hagelaar G J M and Kroesen G M W 2000 *J. Comput. Phys.* **159** 1–12
[34] Whitmer R F and Herrmann G F 1966 *Phys. Fluids* **9** 768–73
[35] Phelps A V ftp://jila.colorado.edu/collision_data/.
[36] Bittencourt J A 1986 *Fundamentals of Plasma Physics* (Oxford: Pergamon)
[37] Parker J H and Lowke J J 1969 *Phys. Rev.* **181** 290–301
[38] Hagelaar G J M and Kroesen G M W 2000 *Plasma Sources Sci. Technol.* **9** 605–14